DALTON
FULL PAPER

Formation kinetics of an aluminium(III)–ethylenedinitrilotetraacetate–fluoride mixed ligand complex ‡

Judit Nemes, Imre Tóth *,† and László Zékány

Department of Inorganic and Analytical Chemistry, Lajos Kossuth University (KLTE), H-4010 Debrecen Pf. 21, Hungary

The formation kinetics of the $[Al(edta)F]^{2-}$ mixed ligand complex has been studied using potentiometric and ^{19}F NMR methods. The rate equation is $-dc_F/dt = d[Al(edta)F^{2-}]/dt = k_1[Al(edta)^-][F^-] + k_2[Al(edta)^-][HF]$, where $k_1 = 20.7 \pm 0.3$ M^{-1} s^{-1} and $k_2 = 471 \pm 93$ M^{-1} s^{-1} at 298 K, the activation parameters for the main reaction path (k_1) being $\Delta H^{\ddagger} = 49.2 \pm 0.9$ kJ mol^{-1}, $\Delta S^{\ddagger} = -54.6 \pm 2.8$ J K^{-1} mol^{-1} studied in the range of pH 4.6–6.0, $T = 283$–328 K and $I = 1$ M $NaNO_3$ medium. An associative interchange (I_a) mechanism can be proposed for the reaction. The stability constant, $K_{AledtaF} = [Al(edta)F^{2-}]/[Al(edta)^-][F^-]$, was redetermined from the kinetic curves: log $K = 4.63 \pm 0.01$ at 298 K, $\Delta H = -25.1 \pm 0.5$ kJ mol^{-1} and $\Delta S = 4.6 \pm 1.5$ J K^{-1} mol^{-1}. The initial rate of the reaction can be used as a kinetic method to determine the aluminium concentration using a fluoride-selective electrode.

Metal–polydentate ligand complexes are important in the migration of metal ions in natural waters[1] and play an essential role in the biodistribution of the metal-containing species in living systems.[2] Multidentate ligands such as the hexadentate ethylenedinitrilotetraacetate (edta) can give rise to unusual coordination geometries,[3] and mixed ligand complexes with metal ions have been observed.[4–6] Equilibrium data for Group 13 of the Periodic Table are available,[7–9] and extensive work motivated by the acid rain problem has been done on aluminium(III) complexes.[10,11] Speciation studies in natural waters have also substantially increased knowledge of the analytical chemistry of aluminium.[12] Although the speciation of metal complexes in multicomponent systems can be related to the rate of equilibration,[13] kinetic information on the main group metals is relatively limited. Solvent exchange mechanisms for Al, Ga and In have been studied.[14] There have been fewer studies for reactions involving the formation of mixed ligand complexes where part of the inner hydration sphere of the metal ion has already been replaced by another ligand or ligand(s). Reactivity patterns of the ternary complexes can be used as models for many catalytic reactions involving the formation and dissociation of metal–donor bonds.[15] The reactions of Al^{III} with mono- and bi-dentate ligands[16a,17] follow the Eigen–Wilkins mechanism, are relatively slow for the $[Al(H_2O)_6]^{3+}$ ions and substantially faster for the $[Al(H_2O)_5(OH)]^{2+}$ ions.

The aim of this study was to determine the mechanism of formation of the mixed ligand $[Al(edta)F]^{2-}$ complex using potentiometry and ^{19}F NMR spectroscopy. A kinetic method to measure aluminium concentration using a fluoride-selective electrode was also developed.

Experimental

Materials

A stock solution of K[Al(edta)] (0.05 M) was prepared from $Al(NO_3)_3$ (p.a. Reanal) and K_2H_2edta. The K_2H_2edta solution was made from H_4edta (p.a. Reanal) and KOH. In order to avoid the presence of free Al^{III}, 5% excess of edta was used. The pH was adjusted to 4 by adding concentrated KOH. The stock solutions were prepared at least 1 d before the kinetic experiments giving enough time for equilibration. Sodium fluoride (p.a. Reanal) was recrystallized in water and a weighed amount of the solid was dissolved in doubly distilled water. The 0.100 M NaF stock solution was kept in a plastic vessel.

Kinetic procedures

Potentiometry. A measuring cell consisting of a Radelkis OP-F-0711 P fluoride-selective electrode and a Radelkis OP-0830 P saturated calomel electrode was used to monitor the fluoride concentration in the reaction mixture. In each run a solution (20 cm^3) containing NaF, 0.05 M acetic acid–sodium acetate buffer§ and 1 M $NaNO_3$ ionic medium (adjusted to the required pH by adding concentrated HCl or NaOH) was thermostatted in a plastic titration vessel at the desired temperature. The NaF solution was stirred by a Teflon coated magnetic stirring bar. The $[Al(edta)]^-$ solution was then injected with an automatic pipette and the potential measured against time. The response time of the measuring electrode was checked and found[16a,b] to be less than 1 s, therefore it was possible to follow the relatively slow formation reaction of the mixed ligand complex, $[Al(edta)F]^{2-}$.

The initial fluoride concentration (c_F^0) ranged from 1×10^{-5} to 2×10^{-4} M. In order to keep the pseudo-zero-order condition for $[Al(edta)]^-$ a minimum 10-fold excess of the complex (c_{Aledta}^0) over the initial total fluoride (c_F^0) was maintained. Reactions were studied at different pH from 4.6 to 6.0 and temperatures, 283, 298, 308 and 323 K. The studied pH region was limited by the lower selectivity of the measuring electrode at pH > 6 because of the interference of hydroxide ions and by the limited buffer capacity of the acetate–acetic acid system. At pH ≤ 4.2 the dissociation of the $[Al(edta)]^-$ complex can occur in the presence of fluoride resulting in the formation of $[AlF_x]^{3-x}$ complexes.

The electromotive force (E) was measured by a Radelkis OP-208/1 digital pH-meter. Calibration of the measuring cell was done by titration of 1 M $NaNO_3$ containing 0.05 M acetic acid–sodium acetate buffer by NaF. The slope of the E *vs.* log c_F curve was almost theoretical in the range of log $c_F = 2$–5.5 and the drift of the intercept was measured to be less than 1 mV for

† E-Mail: itoth@tigris.klte.hu

‡ *Supplementary data available*: primary kinetic data, equilibrium constants. For direct electronic access see http://www.rsc.org/suppdata/dt/1998/2707/, otherwise available from BLDSC (No. SUP 57408, 11 pp.) or the RSC Library. See Instructions for Authors, 1998, Issue 1 (http//www.rsc.org/dalton).

§ Acetate forms weak complexes with Al^{3+}. The negligible effect of the acetate has been checked, *e.g.* the ^{19}F NMR shift of $[Al(edta)F]^{2-}$ was found to be equal in the presence and absence of the buffer.

calibration curves recorded before and after the kinetic runs. The same pH-meter was used to measure the pH with a GK2421C combination pH-electrode (Radiometer) calibrated to standard buffers. The reading was corrected using the method by Irving *et al.*[18] The method of calibration gives the concentration (M) of F^- and H^+, therefore the equilibrium constants calculated from the *E* values are stoichiometric values.

^{19}F NMR Studies. The ^{19}F NMR spectra were recorded by a Bruker DRX 500 spectrometer at 470.26 MHz. Typical acquisition parameters were: 7 μs (70°) pulse length, spectral window = 10–70 ppm, data points = 16 K, relaxation delay 2 s. Chemical shift values are referred to a 0.05 M NaF solution (pH 12, 10% D_2O), δ 0. Selective magnetization transfer experiments were carried out using a DANTE pulse train.[19] The observed signals are in the 'slow exchange' regime and the line broadening can be used to evaluate the pseudo-first-order rate constants by the formula $k_{obs} = \pi(\Delta\nu_{\frac{1}{2}}^{obs} - \Delta\nu_{\frac{1}{2}}^{0})$, where $\Delta\nu_{\frac{1}{2}}^{obs}$ is measured and $\Delta\nu_{\frac{1}{2}}^{0}$ is the non-exchange linewidth for the signal. The limit of the measurable rate constants can be calculated from the accuracy of the linewidth measurements;[20] in our case $(\Delta\nu_{\frac{1}{2}}^{obs} - \Delta\nu_{\frac{1}{2}}^{0}) \geqslant 3$ Hz could be estimated, thus reactions with $k_{obs} \geqslant 10$ s^{-1} give measurable broadening. The lack of measurable exchange broadening in ^{19}F NMR is a clear indication of fairly slow kinetics. The magnetization transfer (MT) method extends the timescale to slower reactions. In the present case the typical transverse relaxation time (T_1) of ^{19}F NMR signals is about 1.5 s, therefore chemical exchange processes having $k_{obs} \geqslant 0.2$ s^{-1} (or average lifetimes, $\tau = 1/k_{obs} \leqslant 3T_1 \approx 5$ s) can be followed by MT.

Data treatment

Pseudo-first-order rate constants. The potential of the measuring cell is defined by equation (1) where $m = 2.303(RT/F)$, A',

$$E = A' - m\log[F^-] = \{A' + m\log(1 + K_{HF}[H^+])\} - m\log c_F = A - m\log c_F \quad (1)$$

A are the intercepts, respectively, and c_F is given by equation (2)

$$c_F = [F^-] + [HF] = [F^-] + K_{HF}[H^+][F^-] = (1 + K_{HF}[H^+])[F^-] \quad (2)$$

where $K_{HF} = [HF]/[H^+][F^-] = 10^{2.90}$ is the protonation constant[21] of fluoride at $I = 1$ M. The rate of F^- consumption can be evaluated from the *E vs.* time (*t*) plot. If the pH is constant at $t = 0$ differentiation of equation (1) gives the initial rate (3).

$$\left(\frac{dE}{dt}\right)_{t=0} = -\frac{m}{2.303}\cdot\frac{1}{[F^-]_{t=0}}\cdot\left(\frac{d[F^-]}{dt}\right)_{t=0} = -\frac{m}{2.303}\cdot\frac{1}{c_F^{(t=0)}}\cdot\left(\frac{dc_F}{dt}\right)_{t=0} \quad (3)$$

Rearrangements give the pseudo-first-order rate constant k_{obs}, equation (4), where c_F^0 is the starting value at $t = 0$. Values of

$$k_{obs} = \frac{2.303}{m}\cdot\left(\frac{dE}{dt}\right)_{t=0} = -\frac{1 + K_{HF}[H^+]}{c_F^0}\cdot\left(\frac{d[F^-]}{dt}\right)_{t=0} = -\frac{1}{c_F^0}\cdot\left(\frac{dc_F}{dt}\right)_{t=0} \quad (4)$$

$(dE/dt)_{t=0}$ can be determined by drawing a tangent to the initial part of the plots of *E vs.* time data. This approximation was used to check the order of the reaction in F^- and $[Al(edta)]^-$.

The kinetic curves were also fitted using a second-order reversible model ($A + B \rightleftharpoons AB$). At constant pH values (in buffer) the reactions of protonated/deprotonated species are indistinguishable, therefore the concentrations in equations (5) and (6) were used in the rate equation, c_{Aledta}^0 is the starting

$$c_{Aledta} = [Al(edta)^-] + [Al(edta)(OH)^{2-}] = (1 + K_{AledtaOH}/[H^+])[Al(edta)^-] = c_{Aledta}^0 - c_{AledtaF} \quad (5)$$

$$c_{AledtaF} = [Al(edta)F^{2-}] = c_F^0 - c_F \quad (6)$$

value at $t = 0$, $K_{AledtaOH} = [Al(edta)(OH)^{2-}][H^+]/[Al(edta)^-] = 10^{-5.81}$ M (see refs. 4 and 7). Using the conditional rate constants of the second-order formation (k_f) and the first-order dissociation (k_d) reaction of the mixed ligand complex $[Al(edta)F]^{2-}$ the rate equation (7) can be written. Substitution of equations

$$\frac{dc_{AledtaF}}{dt} = -\frac{dc_F}{dt} = \frac{2.303}{m}\cdot\frac{dE}{dt}\cdot c_F = k_f c_{Aledta} c_F - k_d c_{AledtaF} \quad (7)$$

(5) and (6) into (7) gives the differential equation (8) which can

$$-\frac{dc_F(t)}{dt} = k_f[c_{Aledta}^0 - c_F^0 + c_F(t)]c_F(t) - k_d[c_F^0 - c_F(t)] \quad (8)$$

be solved explicitly with the initial condition $c_F(0) = c_F^0$. Replacing the k_f constant from $k_{obs} = k_f c_{Aledta}^0$ and introducing a conditional equilibrium constant, $K_{obs} = k_{obs}/(k_d c_{Aledta}^0) = k_f/k_d$, the solution can be written as in equation (9); ξ is the conversion of the reversible reactions and its value is slightly lower than 1. Least squares fitting of the data points can be made for the *E vs. t* plots using equation (12).

$$c_F(t) = c_F^0 f(t, k_{obs}, K_{obs}, c_F^0, c_{Aledta}^0) = c_F^0\left[1 - \frac{\xi(1 - e^{-Qk_{obs}t})}{1 - (1 - Q\xi)e^{-Qk_{obs}t}}\right] \quad (9)$$

$$Q = \sqrt{\left(1 + \frac{1}{K_{obs}c_{Aledta}^0} - \frac{c_F^0}{c_{Aledta}^0}\right)^2 + \frac{4c_F^0}{K_{obs}(c_{Aledta}^0)^2}} \quad (10)$$

$$\xi = \frac{2}{1 + \frac{1}{K_{obs}c_{Aledta}^0} + \frac{c_F^0}{c_{Aledta}^0} + Q} \quad (11)$$

$$E_t = A - \log c_F(t) = (A - \log c_F^0) - \log f(t) = E_0 - \log f(t, k_{obs}, K_{obs}, c_F^0, c_{Aledta}^0) \quad (12)$$

Three parameters have been estimated: E_0 is the intercept at $t = 0$ (which cannot be substantially different from the starting value), k_{obs} and K_{obs}. The latter can be used to estimate the stoichiometric stability constant of the mixed ligand complex $[Al(edta)F]^{2-}$ (see below); ±0.2–1.7% accuracy of k_{obs} has been found for the fitting procedure.

Rate equation. The total rate of the complex formation might be described for the three (dominating) reactions (19)–(21) (see below) by equation (13) where [HF] and $[Al(edta)(OH)^{2-}]$ can

$$-dc_F/dt = k_1[Al(edta)^-][F^-] + k_2[Al(edta)^-][HF] + k_3[Al(edta)(OH)^{2-}][F^-] \quad (13)$$

be eliminated by using K_{HF} and $K_{AledtaOH}$. Rearrangement using (2) and (5) eliminates $[Al(edta)^-]$ and $[F^-]$ giving equation (14).

$$-\frac{dc_F}{dt} = \frac{k_1 + k_2K_{HF}[H^+] + k_3K_{AledtaOH}[H^+]^{-1}}{(1 + K_{AledtaOH}[H^+]^{-1})(1 + K_{HF}[H^+])}\cdot c_{Aledta}c_F \quad (14)$$

Dividing the rate by c_F, and substituting c_{Aledta}^0 (c_{Aledta} at $t = 0$) into (14) gives the pseudo-first-order rate constant, equation (15). Note, there are only constants and $[H^+]$ in equation (15).

$$k_{obs} = \frac{k_1 + k_2K_{HF}[H^+] + k_3K_{AledtaOH}[H^+]^{-1}}{(1 + K_{AledtaOH}[H^+]^{-1})(1 + K_{HF}[H^+])} \cdot c^0_{Aledta} \quad (15)$$

This function was least squares fitted to the measured values of k_{obs} *vs.* pH, the estimated parameters being k_1, k_2 and k_3. Weighting by the error of k_{obs} found in the fitting procedure according to equation (12) was used. The temperature dependence of values of k_i can yield the activation parameters of the reactions using the Eyring formula (16). In order to check the

$$\log \frac{k_i}{T} = 10.319 + \frac{1}{2.303R} \cdot \left(\Delta S_i^{\ddagger} - \frac{\Delta H_i^{\ddagger}}{T} \right) \quad (16)$$

reliability of the activation parameters all data points of the temperature and pH variation measurements were also fitted together by equations (15), (16) and (18) (see below).

Equilibrium constant. All measurements have been directed to obtaining kinetic information. The pseudo-first-order condition for $[Al(edta)]^-$ means that at equilibrium, or in other words at $t = t_\infty$, the ratio $[Al(edta)F^-]:[F^-]$ is very high. This condition is far from optimal for determining the stoichiometric equilibrium constant of the mixed ligand complex. Nevertheless, the pH dependence of $K_{obs} = k_{obs}/k_d c^0_{Aledta} = k_f/k_d$ can be used to calculate the stability constant. After rearrangements using (2) and (5) the conditional stability constant at $t = t_\infty$ can be written as in equation (17). The log K_{obs} *vs.* pH curves were least

$$K_{obs} = \frac{c^\infty_{AledtaF}}{c^\infty_{Aledta} c^\infty_F} = \frac{K_{AledtaF}}{(1 + K_{AledtaOH}[H^+]^{-1})(1 + K_{HF}[H^+])} \quad (17)$$

squares fitted using $K_{AledtaF}$ as an estimated parameter. The formation enthalpy and entropy of the $[Al(edta)F]^{2-}$ mixed ligand complex were evaluated by equations (17) and (18),

$$\log K = \frac{1}{2.303R} \cdot \left(\Delta S - \frac{\Delta H}{T} \right) \quad (18)$$

fitting together the data of pH and temperature dependence measurements. The least squares fitting of the data points was done using a program written in MATLAB (The Math Works, Inc.). Uncertainties are given as 1σ throughout the paper.

Results and Discussion

The speciation of the H^+–Al^{III}–$edta^{4-}$–F^- system has been studied.[4,6,7] Typical distribution curves can be seen in Fig. 1. The equilibrium system is simple as there are only three aluminium complexes: (1) $[Al(edta)]^-$, (2) the deprotonated form $[Al(edta)(OH)]^{2-}$ and (3) the mixed ligand complex $[Al(edta)F]^{2-}$. There is no H[Al(edta)] complex present in the system at this pH. The stability of the mixed ligand complex is high, therefore the concentration of free fluoride at equilibrium is quite low, and the ratio of $[F^-]:[HF]$ is governed by the pH.¶ The ^{19}F NMR spectra show two signals at δ −49.2 and −2.2 for $[Al(edta)F]^{2-}$ and free F^-/HF, respectively (Fig. 2). The chemical shift and the linewidth of the mixed ligand complex is constant; the signal of the free fluoride is slightly shifted at higher excess of fluoride because of a small increase of pH, but it has also a constant linewidth.

Rate equation

The reaction of $[Al(edta)]^-$, $[Al(edta)(OH)]^{2-}$ and H[Al(edta)] with fluoride ligand present either as F^- or HF results in

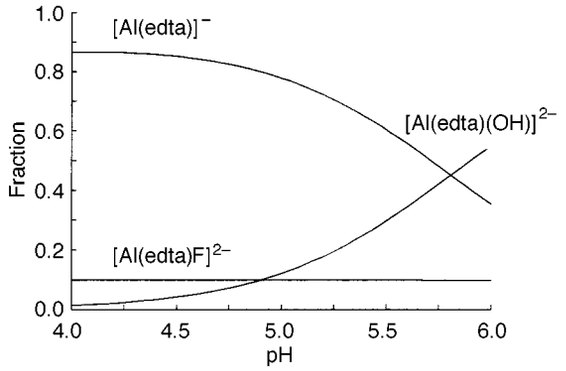

Fig. 1 Typical distribution curves in the Al^{III}–$edta^{4-}$–F^-–H^+ system: c_{Al} = 2 mM, c_{edta} = 2.1 mM, c_F = 0.2 mM

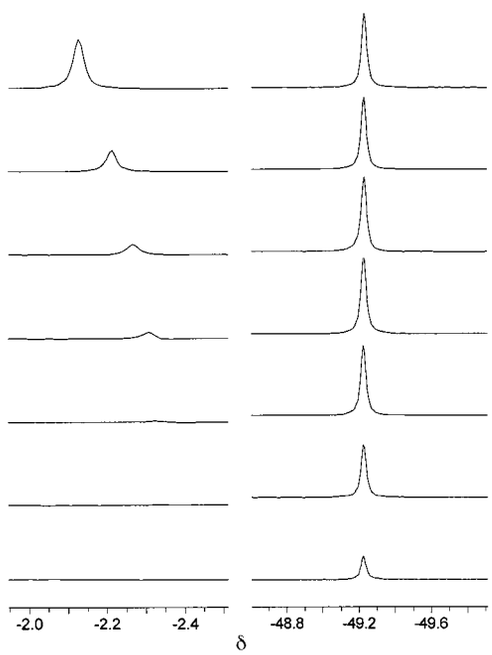

Fig. 2 Typical ^{19}F NMR spectra measured at c_{Al} = 5.00 mM, c_{edta} = 5.5 mM, pH 4.7 ± 0.1 in 50 mM acetate buffer. $\delta_{AledtaF}$ −49.2 and $\delta_{F/HF} \approx$ −2.2. c_F (mM) varies upwards: 1.0, 2.0, 3.0, 4.0, 5.0, 7.0 and 10.0

the formation of the mixed ligand complex, $[Al(edta)F]^{2-}$. Only three of the six possible reactions, (19)–(21), have to be

$$[Al(edta)]^- + F^- \underset{k_{-1}}{\overset{k_1}{\rightleftharpoons}} [Al(edta)F]^{2-} \quad (19)$$

$$[Al(edta)]^- + HF \underset{k_{-2}}{\overset{k_2}{\rightleftharpoons}} [Al(edta)F]^{2-} + H^+ \quad (20)$$

$$[Al(edta)(OH)]^{2-} + F^- \underset{k_{-3}}{\overset{k_3}{\rightleftharpoons}} [Al(edta)F]^{2-} + OH^- \quad (21)$$

considered, as only these have both reactants coexisting in significant concentration in the studied pH region. The equilibrium constants of the reversible reactions are $K_{AledtaF} = [Al(edta)F^{2-}]/[Al(edta)^-][F^-] = 10^{4.8}$ M^{-1} for (19),[4] $K'_{AledtaF} = [Al(edta)F^{2-}][H^+]/[Al(edta)^-][HF] = K_{AledtaF}/K_{HF} = 10^{1.9}$ for (20) and $K''_{AledtaF} = [Al(edta)F^{2-}][OH^-]/[Al(edta)(OH)^{2-}][F^-] = K_{AledtaF}K_w/K_{AledtaOH} = 10^{-3.2}$ for (21), the ionic product of water[4] being $K_w = 10^{-13.83}$ M^2. The deprotonation of $[Al(edta)]^-$, or in other words the proton exchange, is very fast and may be diffusion controlled. The proton exchange in the HF–F^-–H_2O system is not as fast[22,23] as it is for the hydrolysis of $[Al(edta)]^-$, but fast enough compared to the reactions (19)–(21) not to be considered as the rate determining step.

In order to determine the order of the reaction in $[Al(edta)]^-$

¶ At lower pH and at large excess of fluoride the dissociation of $[Al(edta)]^-$ takes place resulting in the formation of binary complexes $[AlF_x]^{(3-x)+}$ and $H_nedta^{(4-n)-}$.

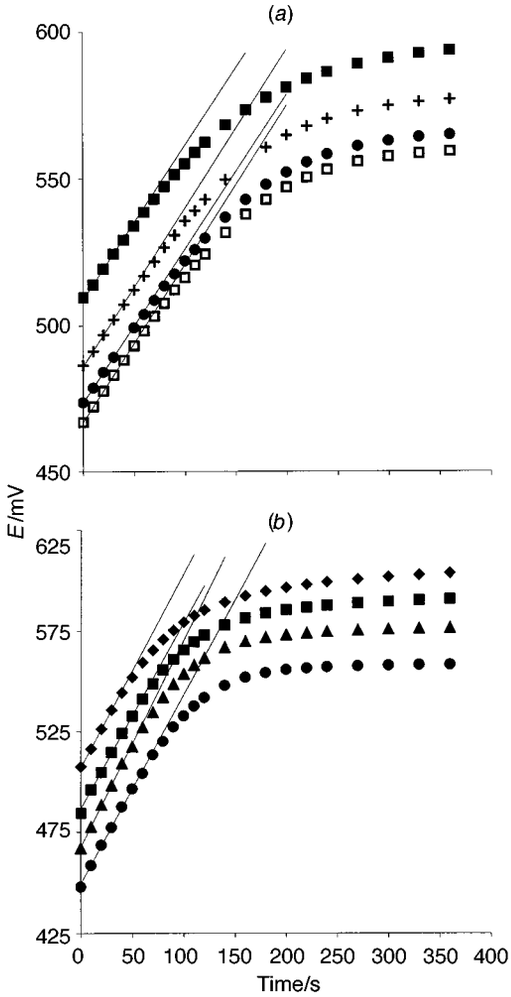

Fig. 3 Initial rate of formation of the $[Al(edta)F]^{2-}$ mixed ligand complex at 298 K, pH 5.05. Symbols show the experimental values. (*a*) $c^0_{Aledta} = 1.00 \times 10^{-3}$ M, $10^5 c^0_F$/M 2.00 (■), 5.00 (+), 8.00 (●) and 10.0 (□); (*b*) $c^0_{Aledta} = 2.00 \times 10^{-3}$ M, $10^5 c^0_F$/M 2.00 (◆), 5.00 (■), 8.00 (▲) and 10.0 (●). Tangents have been drawn using three potential values measured at $t = 10$, 20 and 30 s. The potential values measured at $t = 0$ s were not used because they can be somewhat different from the values measured in the slightly diluted solution after the injection of the [Al(edta)] stock solution

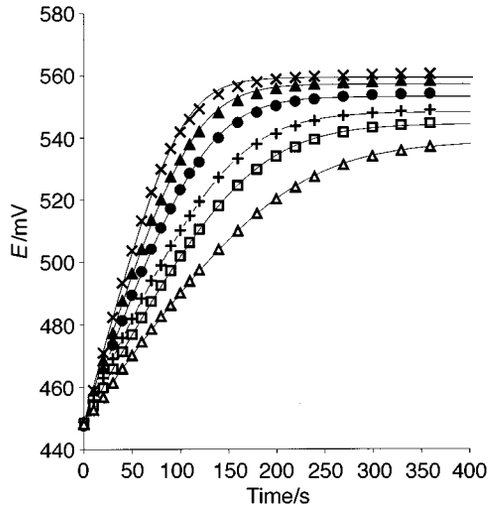

Fig. 4 pH Dependence of the rate of formation of $[Al(edta)F]^{2-}$. $c^0_{Aledta} = 2.00 \times 10^{-3}$ M, $c^0_F = 2.00 \times 10^{-4}$ M, $T = 298$ K. Symbols show the measured values at different pH: 4.84 (×), 5.06 (▲). 5.28 (●), 5.57 (+), 5.74 (□) and 5.93 (△). The lines have been computed by equation (12). Estimated values of k_{obs} and K_{obs} are summarized in Table 1

and F^-, kinetic runs were done at different values of both c^0_{Aledta} and c^0_F. Typical experimental curves are shown in Fig. 3(*a*) and 3(*b*). The initial parts of the kinetic curves recorded at constant c^0_{Aledta} and different c^0_F [Fig. 3(*a*)] were found to be parallel, therefore the k_{obs} values derived from the slopes are equal within the experimental errors ($k_{obs} = 2.07 \times 10^{-2}$ s^{-1}, average of four curves), indicating first-order kinetics in $[F^-]$. Values of k_{obs} at double the concentration of $[Al(edta)]^-$, c^0_{Aledta} [Fig. 3(*b*)], were about two times larger ($k_{obs} = 3.76 \times 10^{-2}$ s^{-1}, average of four curves), therefore the reaction is also first order in $[Al(edta)^-]$.

The complete description of the kinetic curves using a second-order reversible model gives the values of k_{obs} and K_{obs} according to the formula (12). The least squares fitted parameters are shown in Table 1.

The contributions of the three reaction paths (19)–(21) were determined by the pH dependence of the reaction rate at 298 K as shown in Fig. 4. The same experiments were also carried out at 283, 308 and 323 K (see SUP 57408).

The best fit using equation (15) for the k_{obs} *v.s.* pH curves was found in a trial, where at log $K_{AledtaOH} = -5.8$ (fixed) and log $K_{HF} = 2.90$ (fixed) two reactions, (19) and (20), were involved in the model. (Calculations with only k_1 resulted in significantly larger deviations especially at lower pH values. In a model with $k_1 + k_3$ a negative value of k_3 could be estimated.) Parameter fitting was done in two different ways. (1) Using values of six to seven k_{obs} measured at given temperatures, values of $k_1 = 7.10 \pm 0.13$ (283), 20.7 ± 0.3 (298), 43.3 ± 0.7 (308) and 105.4 ± 1.6 (328 K) M^{-1} s^{-1}, $k_2 = 194 \pm 37$ (283), 471 ± 93 (298), 371 ± 116 (308) and 953 ± 309 (328 K) M^{-1} s^{-1} were computed. The uncertainty of k_2 is quite large, while k_1 can be estimated with high accuracy. The temperature dependence of k_1 values according to the Eyring equation (16) gives $\Delta H^\ddagger = 49.2 \pm 0.9$ kJ mol^{-1}, $\Delta S^\ddagger = -54.6 \pm 2.8$ J K^{-1} mol^{-1} for the reaction (19). The results are presented in Fig. 5. (2) The values of 26 k_{obs} have been fitted together using equations (15) and (16). Four parameters were estimated; values of log $K_{AledtaOH}$ and log K_{HF} were fixed. The estimated parameters were very similar to those above: k_1 (298 K) $= 21.1 \pm 0.2$ M^{-1} s^{-1}, $\Delta H^\ddagger = 49.5 \pm 0.5$ kJ mol^{-1}, $\Delta S^\ddagger = -53.4 \pm 1.8$ J K^{-1} mol^{-1} and k_2 (298 K) $= 355 \pm 59$ M^{-1} s^{-1}. No reliable activation parameters can be estimated for reaction (20).

Although reaction (19) is certainly the dominating one for the formation of the mixed ligand complex, (20) seems to be in action at the lower pH values. We note that the contribution of reaction (20) is small. At pH ⩾ 5 it amounts to a few percent and never exceeds 25%, as can be seen in Fig. 6. The pH region cannot be extended to lower values because of the dissociation of the $[Al(edta)]^-$ (see above).

Reaction (20) cannot be distinguished from the reaction between H[Al(edta)] + F^-, which shows the same pH dependence, and it could also contribute simultaneously to the formation of the mixed ligand complex. Nevertheless it seems to be less favourable from the equilibrium point of view in the studied pH range. Although the dissociation of M(edta) complexes, *e.g.* M = lanthanide(III) ion, can be proton catalysed[5] resulting in a faster rate of the central ion exchange[5a] or ligand exchange[5b] reactions, the mixed ligand complex formation[24] with H[Ru(edta)] is less favored compared to that with $[Ru^{III}(edta)]^-$. The same considerations are valid for the reaction between $[Al(edta)(OH)]^{2-}$ and HF, *i.e.* it is indistinguishable from the reaction between $[Al(edta)]^-$ and F^-.

The absence of the reaction of $[Al(edta)(OH)]^{2-}$, which is a major species at higher pH, see Fig. 1, with F^- needs further discussion. In principle, all rate constants can also be evaluated from ^{19}F NMR magnetization transfer experiments. We attempted to detect some exchange reactions in a sample prepared at the highest possible pH where the mixed ligand complex can still exist. The composition of the sample was as

Table 1

T/K	pH	k_{obs}/s^{-1}	log K_{obs}	E_0/mV	st.d.* of E/mV
283.4	4.597	0.0190 ± 0.7%	4.862 ± 0.008	438.57 ± 0.33	0.78
	4.822	0.0179 ± 0.9%	4.838 ± 0.009	439.67 ± 0.39	0.95
	5.027	0.0150 ± 0.5%	4.775 ± 0.005	438.67 ± 0.22	0.43
	5.336	0.0123 ± 0.4%	4.753 ± 0.005	436.63 ± 0.18	0.44
	5.530	0.0103 ± 0.6%	4.647 ± 0.007	437.72 ± 0.20	0.53
	5.710	0.0080 ± 0.2%	4.582 ± 0.003	438.08 ± 0.07	0.18
	6.051	0.0053 ± 0.2%	4.476 ± 0.011	438.10 ± 0.03	0.08
298.2	4.837	0.0467 ± 1.0%	4.616 ± 0.010	448.39 ± 0.54	0.90
	5.058	0.0398 ± 0.8%	4.571 ± 0.008	448.82 ± 0.43	0.75
	5.353	0.0345 ± 0.7%	4.517 ± 0.006	447.94 ± 0.35	0.62
	5.566	0.0271 ± 0.5%	4.409 ± 0.004	449.27 ± 0.23	0.43
	5.740	0.0234 ± 0.4%	4.358 ± 0.003	448.37 ± 0.15	0.30
	5.933	0.0180 ± 0.4%	4.264 ± 0.003	448.16 ± 0.14	0.30
308.2	4.604	0.0956 ± 1.2%	4.478 ± 0.010	455.18 ± 0.58	0.74
	4.813	0.0841 ± 1.1%	4.449 ± 0.009	455.26 ± 0.56	0.74
	5.035	0.0794 ± 1.0%	4.431 ± 0.009	454.56 ± 0.50	0.67
	5.310	0.0662 ± 1.0%	4.376 ± 0.008	453.40 ± 0.48	0.68
	5.727	0.0464 ± 0.6%	4.226 ± 0.004	452.69 ± 0.25	0.39
	6.051	0.0325 ± 0.4%	4.066 ± 0.003	453.09 ± 0.16	0.26
323.2	4.622	0.2310 ± 1.7%	4.267 ± 0.012	461.18 ± 0.72	0.74
	4.820	0.2104 ± 1.5%	4.249 ± 0.011	461.27 ± 0.66	0.69
	5.028	0.1971 ± 1.6%	4.227 ± 0.011	460.43 ± 0.66	0.70
	5.322	0.1560 ± 1.2%	4.152 ± 0.008	460.54 ± 0.48	0.52
	5.541	0.1358 ± 1.1%	4.083 ± 0.007	461.38 ± 0.42	0.46
	5.716	0.1156 ± 1.0%	4.017 ± 0.006	461.22 ± 0.37	0.42
	6.015	0.0833 ± 0.6%	3.864 ± 0.003	460.08 ± 0.18	0.22

* st.d. of E is $[\sum_{i=1}^{n}(E_{meas(i)} - E_{calc(i)})^2/(n_{exp} - n_{par})]^{\frac{1}{2}}$ where n_{exp} is the number of experimental points and n_{par} the number of estimated parameters.

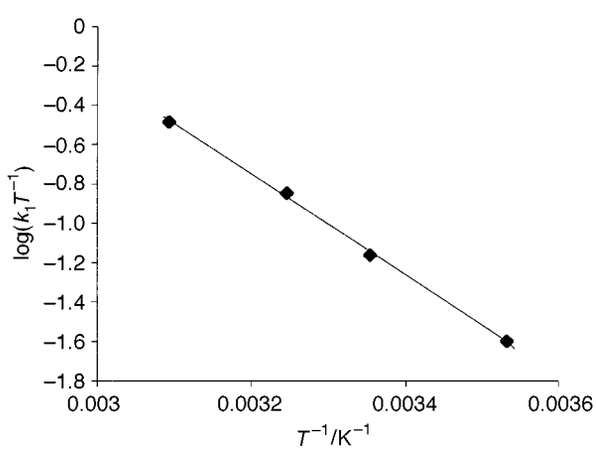

Fig. 5 Eyring plot for the reaction (19)

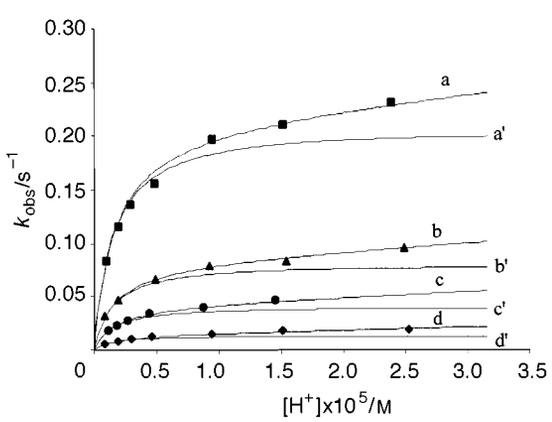

Fig. 6 pH Dependence of the reaction rate. Symbols show the experimental values for different temperatures, T/K: 328 (■), 308 (▲), 298 (●) and 283 (◆). The lines have been calculated for the overall reaction ($k_1 + k_2$: a, b, c and d) and for the main reaction (k_1: a′, b′, c′ and d′) at the above temperatures, respectively

follows: 5.00 mM Al^{3+}, 20.0 mM edta, 20.0 mM NaF, pH 9.0: the excess of edta was added to suppress the dissociation of the complex to $[Al(OH)_4]^-$; $[Al(edta)(OH)^{2-}] = 4$ mM, $[Al(edta)F^{2-}] = 1$ mM, $[F^-] = 19$ mM can be calculated in agreement with the measured integral values. At pH 9 the fluoride-selective electrode cannot be used. The contribution of reaction (21) to the formation of the mixed ligand complex, if there is any, could be studied in the absence of the other faster reactions. In fact, no measurable magnetization transfer was observed either at 298 or at 323 K, therefore one can estimate $k_{obs} = -(d[Al(edta)F^{2-}]/dt)/[Al(edta)F^{2-}] = k_{-3}[OH^-] \leqslant 0.2$ s^{-1} (see above). Calculation of the rate constant of the forward reaction (21) gives $k_3 = K''_{AledtaF}\, k_{obs}/[OH^-] \leqslant 9$ M^{-1} s^{-1}. At 323 K values of $k_1 = 105$ and $k_2 = 953$ M^{-1} s^{-1} can be measured by the potentiometric method, therefore substantial contribution of this path (21) can be ruled out even under these extreme conditions.

The MT experiments also show the absence of ligand exchange reaction without net chemical exchange: $[Al(edta)F]^{2-} + {}^*F^- \rightleftharpoons [Al(edta)^*F]^{2-} + F^-$. This is contrary to the AlF_x system ($x = 2$ or 3) where these reactions are relatively fast.[25] The absence of these reactions is an indication of the 'crowded' co-ordination sphere of the Al^{3+} ion in the $[Al(edta)(OH)]^{2-}$ and $[Al(edta)F]^{2-}$ mixed ligand complexes, and the slow rate of the dissociation of the F^- ion from $[Al(edta)F]^{2-}$. Consequently, the experimental rate equation can be written as (22) where $k_2[HF]$ might be replaced by $k_2K_{HF}[H^+][F^-]$. Our

$$-dc_F/dt = d[Al(edta)F^{2-}]/dt = k_1[Al(edta)^-][F^-] + k_2[Al(edta)^-][HF] \quad (22)$$

reasoning to attribute the pH dependence to the reactivity difference between the $[Al(edta)]^-$ and the $[Al(edta)(OH)]^{2-}$ and F^- and HF is based on the following observations. First, two protonation/deprotonation equilibria are needed to explain the pH dependence, and secondly the pH profile of the rate can be described by a constant very similar to $K_{AledtaOH}$ in a trial calculation using $K_{AledtaOH}$ as a fitted parameter. A similar reactivity order has been recognized for $[Ru(edta)]^-$ and $[Ru(edta)(OH)]^{2-}$ reacting with monodentate ligands.[24] It is worth men-

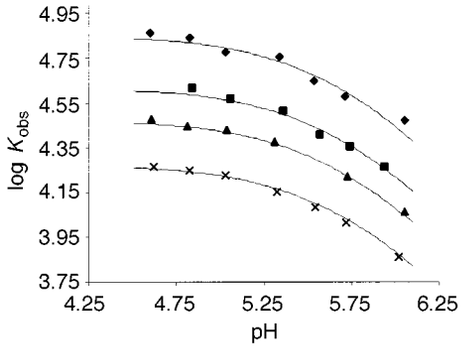

Fig. 7 Determination of the stability constant, $K_{AledtaF}$, of the mixed ligand complex. The symbols show the values of the conditional stability constant, K_{obs}, from the fitting procedure using equation (12) at T/K: 283 (◆), 298 (■), 308 (▲) and 328 (×). The lines represent the calculated values using equations (17) and (18)

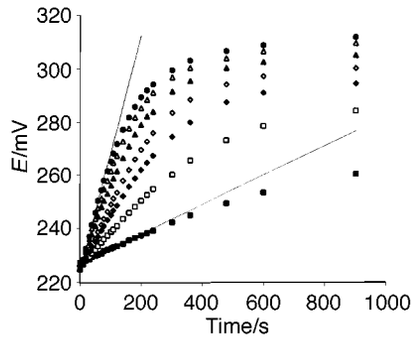

Fig. 8 Kinetic method to measure aluminium concentrations. $c_F^0 = 1.00 \times 10^{-5}$ M, pH 5.01, $T = 298$ K. Symbols show the experimental values at different 10^4 c^0_{Aledta}/M: 8.75 (●), 7.50 (△), 6.25 (▲), 5.00 (◇), 3.75 (◆), 2.50 (□) and 1.00 (■). Only two tangents are shown for clarity; five and five points, measured at $t = 20$, 30, 40, 50 and 60 s, have been used to draw the slopes

tioning that the increased rate of the reaction at lower pH might be attributed to a lower reactivity of F^- compared to that of HF. Generally, stronger nucleophilicity of HA than of A^- is very much unlikely for the weak acids and their anions, but the F^-/HF pair seems to be an exception. Hard metal centers such as Be^{II},[26] Fe^{III} [27] and uranyl(II) [28,29] behave similarly to F^-/HF.

Stability constant

Evaluation of the stoichiometric stability constant, $K_{AledtaF}$, has been done by curve fitting of K_{obs} varying with pH and temperature using equations (17) and (18). Values of 26 K_{obs} were involved in the evaluation, the log $K_{AledtaOH}$ and log K_{HF} constants being fixed. The result can be seen in Fig. 7. The value of log $K_{AledtaF}$ (298 K) = 4.63 ± 0.01 is in good agreement with the values measured earlier.[4,6] Values of $\Delta H = -25.1 \pm 0.5$ kJ mol^{-1} and $\Delta S = 4.6 \pm 1.5$ J K^{-1} mol^{-1} have been estimated for the formation of the mixed ligand complex, but the reliability of these values is limited by the fact that protonation constants ($K_{AledtaOH}$ and K_{HF}) measured at 298 K were used as fixed parameters for the fitting procedure. However, the $[Al(edta)F]^{2-}$ mixed ligand complex is certainly an enthalpy stabilized species contrary to the entropy stabilized AlF_x parent [21] complexes. A similar calculation was done using $K_{AledtaOH}$ as a fitted parameter. It resulted in very similar values: log $K_{AledtaF}$ = 4.64 ± 0.01, $\Delta H = -25.4 \pm 1.1$ kJ mol^{-1}, $\Delta S = 3.6 \pm 3.8$ J K^{-1} mol^{-1}. The log $K_{AledtaOH}$ (298 K) = −5.79 ± 0.02. This hydrolysis constant, which in fact contains K_w, shows only a slight temperature dependence.

Determination of aluminium concentration

The high stability of the mixed ligand complex $[Al(edta)F]^{2-}$, and the simple rate law given by equation (22), give a chance to use the formation reaction as an analytical tool for measuring aluminium concentration by fluoride-selective electrodes. Equation (22) shows that the consumption of fluoride *vs.* time or the reaction rate is first order for both $[Al(edta)]^-$ and F^-. Moreover, the k_{obs} given by equation (15) at constant pH is dependent only on the total aluminium concentration, c^0_{Aledta}. It means that on measuring the kinetic curves under the condition $c^0_{Aledta} \geqslant 10c_F$ (*i.e.* under pseudo-first-order conditions) the slope of the starting linear part of the kinetic curves is dependent only on the aluminium concentration. Typical kinetic curves are shown in Fig. 8. A plot of the measured slopes against the concentration is a straight line, and can be considered as a calibration curve for our 'kinetic method' to measure aluminium concentration. Owing to the good sensitivity of the fluoride-selective electrode, the method can be used down to $c^0_{Aledta} \geqslant 10^{-4}$ M (3 mg dm^{-3}) without elaborate procedures;‖ 2–3% uncertainty can be estimated. An obvious disadvantage of this simple and cheap method is that the aluminium content of the sample has to be transferred to the chemical form of $[Al(edta)]^-$. A suitable excess of edta and acetate buffer has to be used for the pretreatment of natural water samples. Some advantages of our method against the known related methods [12,30] can also be pointed out: (1) the stoichiometry of the reaction is known and simple (1 : 1 for Al : F), (2) Fe^{III} does not interfere, because it forms only a much less stable mixed ligand complex [6,10b] compared to Al^{III} and (3) it is cheap and fast. Further work is required to adapt this method for serial analysis.

‖ The concentration range can be extended down to $c^0_{Aledta} \geqslant 10^{-5}$ M at higher temperature and/or at lower pH.

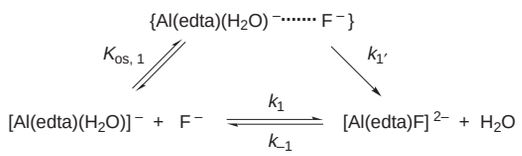

Scheme 1

Mechanistic considerations

Although, an analogy between the formation of the mixed ligand complex $[Al(edta)F]^{2-}$ and the parent $[AlF]^{2+}$ can be expected, the reactivity order of $[Al(edta)]^-$ and $[Al(edta)(OH)]^{2-}$ is the opposite of that of $[Al(H_2O)_6]^{3+}$ and $[Al(H_2O)_5(OH)]^{2+}$. On the other hand, $[Al(edta)]^-$ reacts with F^- about 10 times faster than $[Al(H_2O)_6]^{3+}$ does. This can be attributed to the labilizing effect of the multidentate edta ligand, but this effect is much smaller compared to the effect of one OH^- in $[Al(H_2O)_5(OH)]^{2+}$, which is about 1000 times larger.[16a] It is worth mentioning that the correlation between the stability constant and the reactivity enhancement of co-ordinated water in aluminium(III) complexes, for oxalate and fluoride parent complexes,[31] cannot be extended to the $[Al(edta)(H_2O)]^-$ complex. The experimental finding that $[Al(edta)(OH)]^{2-}$ does not react with F^- shows that no 'additional labilizing effect' of the co-ordinated OH^- has to be considered. Unfortunately, the structure of the $[Al(edta)]^-$(aq) is not known. There is no co-ordinated water in the solid [32] $K[Al(edta)]\cdot 2H_2O$, but co-ordination of one (or two) water ligand(s) has been proposed in aqueous solution.[33] This water ligand can be substituted by F^-/HF. The replacement of OH^- in $[Al(edta)(OH)]^{2-}$ by F^- seems to be both thermodynamically and kinetically less favourable than when H_2O is the leaving ligand.

Although the value of k_2 (20) exceeds that of k_1 (19) by more than one order of magnitude, the formation of the mixed ligand complex $[Al(edta)F]^{2-}$ proceeds dominantly through path (19) throughout the entire pH range studied. We focus our considerations on this dominant accurately measurable reaction. The general formulation of the Eigen–Wilkins [34] mechanism is

shown in Scheme 1. Using the Fouss equation [35] one can calculate the outer sphere stability constant for the ion pair that consists of two −1 charged anions. The crucial point for the calculation is chosing the proper distance of separation of the ions (r) in the outer sphere complex, especially in the case of F^-, which is considered to be a strongly hydrated anion.[36] The generally used value for a single hydration layer in the outer sphere complexes is 5 Å, but for aluminium(III) complexes it ranges from 4.1 [23] to 7.5 Å.[16a] The double hydration layer for the Al^{3+}(aq) cation having well defined first [37] and second hydration spheres [38] seems to be justified, but in the case of the anionic $[Al(edta)]^-$(aq) complex a monolayer should be more reasonable. Based on results of Monte-Carlo simulations and molecular dynamics calculations [39] an estimation of 2.6 Å was made for the distance $F^- \cdots O$ in aqueous solution. Together with the radius of Al^{3+} (0.54 Å) and the radius of water (0.96 Å), a distance of 4.1 Å between the metal center of the complex and the reactant (the Al–H_2O–F unit) has been suggested.[23] In our calculation $r = 4.1$ Å has been used; the calculated $K_{os,1} = 0.052$ M for charges −1, −1. If the condition $K_{os,1}[F^-] \ll 1$ is fulfilled in the pre-equilibrium, the rate of the 'bottleneck' first-order reaction is, $k_1' = k_1/K_{os,1}$, which yields $k_1' = 21.1/0.052 = 406\ s^{-1}$ at 298 K. This elementary reaction could be the leaving of H_2O from the outer sphere complex (D mechanism) or the entering of the F^- into it (A mechanism), but a concerted process (I mechanism) should also be considered. The experimental data are not sufficient to decide unequivocally between the mechanisms. Nevertheless, consideration of the structural information and the activation parameters can lead to a 'qualified guess' of the mechanism. The activation parameters, namely the moderate enthalpy value ($\Delta H^{\ddagger} = 49.2 \pm 0.9$ kJ mol^{-1}) and the negative activation entropy ($\Delta S^{\ddagger} = -54.6 \pm 2.8$ J K^{-1} mol^{-1}), for the reaction (19) lead to the conclusion that the transition state is more ordered compared to the initial state, *i.e.* an associative interchange (I_a) mechanism can be proposed.

The reaction of $[Al(edta)(H_2O)]^-$ with HF, or in other words the proton catalysed reaction with F^-, can be explained by an intermediate consisting of both H_2O and HF. A proton transfer from the entering HF to the water molecule in the intermediate can help the leaving of the water molecule as H_3O^+. The importance of the proton transfer was clearly demonstrated in the UO_2^{2+}–F^-/HF system [28,29] by an inverse isotopic effect in D_2O.

It is interesting to compare our results with those for other metal–aminopolycarboxylate mixed ligand complexes. The formation rate of $[Co(cdta)(CN)]^{3-}$ (cdta = cyclohexane-1,2-diyldinitrilotetraacetate) is much faster [40] than expected from the water exchange rate of $[Co(H_2O)_6]^{2+}$. The suggested mechanism is associative (A). On the contrary, the $[Eu(cdta)]^-$–iminodiacetate [41] and $[Tl(edta)]^-$–X^- (X = Cl, Br, CN or SCN) [42] systems follow a dissociative interchange mechanism (I_d). The kinetics of the $[Al(edta)]^-$–F^- system seems to lie halfway between these reactions: from our experiments an associative interchange (I_a) mechanism can be proposed for the formation of $[Al(edta)F]^{2-}$.

Acknowledgements

This work was supported by the Hungarian National Research Foundation (OTKA 014075 and 026115). The authors thank our friends, Drs. István Bányai (KLTE, Debrecen), Professor Ingmar Grenthe, Zoltán Szabó (KTH, Stockholm) and Michael Read, for helpful discussions.

References

1 W. Stumm and J. J. Morgan, *Aquatic Chemistry*, Wiley, New York, 1981.
2 *Methods Involving Metal Ions and Complexes in Clinical Chemistry*, ed. H. Sigel, Metal Ions in Biological Systems 16, Marcel Dekker, New York, 1983.
3 A. A. McConnell, R. H. Nuttall and D. M. Stalker, *Talanta*, 1978, **25**, 425; R. H. Nuttall and D. M. Stalker, *Talanta*, 1977, **24**, 355.
4 I. Tóth, E. Brücher, L. Zékány and V. Veksin, *Polyhedron*, 1989, **8**, 2057; R. Király, I. Tóth and E. Brücher, *J. Inorg. Nucl. Chem.*, 1981, **43**, 345.
5 (*a*) E. Brücher and P. Szarvas, *Inorg. Chim. Acta*, 1970, **4**, 632; (*b*) E. Brücher and I. Bányai, *J. Inorg. Nucl. Chem.*, 1980, **42**, 749.
6 A. Yuchi, H. Hotta, H. Wada and G. Nakagawa, *Bull. Chem. Soc. Jpn.*, 1987, **60**, 1379; A. Yuchi, K. Ueda, H. Wada and G. Nakagawa, *Anal. Chim. Acta*, 1986, **186**, 313.
7 G. Anderegg, *Critical Survey of Stability Constants of EDTA Complexes*, IUPAC Chemical Data Series, No. 14, Pergamon, Oxford, 1977.
8 R. M. Smith and A. E. Martell, *Critical Stability Constants*, vol. 6, Second Supplement, Plenum Press, New York, 1989.
9 E. Högfeldt, *Stability Constants of Metal-Ion Complexes*, Part A: Inorganic Ligands, IUPAC Chemical Data Series, Pergamon, Oxford, 1982.
10 (*a*) R. J. P. Williams, *Coord. Chem. Rev.*, 1996, **141**, 1; (*b*) R. B. Martin, *Coord. Chem. Rev.*, 1996, **141**, 23.
11 L.-O. Öhman and S. Sjöberg, *Coord. Chem. Rev.*, 1996, **141**, 33.
12 N. Clarke, G. Danielsson and L. Sparén, *Pure Appl. Chem.*, 1996, **68**, 1597.
13 R. W. Smith, *Coord. Chem. Rev.*, 1996, **141**, 81.
14 A. E. Merbach, *Pure Appl. Chem.*, 1982, **21**, 1479.
15 D. N. Hague and A. R. White, *J. Chem. Soc., Dalton Trans.*, 1994, 3645.
16 (*a*) B. J. Plankey and H. H. Pattersson, *Inorg. Chem.*, 1989, **28**, 4331; (*b*) K. Surinivisan and G. A. Rechnitz, *Anal. Chem.*, 1968, **40**, 1818.
17 B. Perlmutter-Hayman and E. Tapuhi, *Inorg. Chem.*, 1977, **16**, 2742.
18 H. M. Irving, M. G. Miles and L. P. Pettit, *Anal. Chim. Acta*, 1967, **38**, 475.
19 A. L. Morris and R. J. Freeman, *Magn. Reson.*, 1978, **29**, 433.
20 J. Sandström, *Dynamic NMR Spectroscopy*, Academic Press, London, 1982.
21 A. M. Bond and G. T. Hefter, *Critical Survey of Stability Constants and Related Thermodynamic Data of Fluoride Complexes in Aqueous Solution*, IUPAC Chemical Data Series, No. 27, Pergamon, Oxford, 1980.
22 M. Eigen and K. Kustin, *J. Am. Chem. Soc.*, 1960, **82**, 5952.
23 P. Zbinden, Ph.D. Thesis, Lausanne, 1994.
24 T. Matsubara and C. Creutz, *Inorg. Chem.*, 1979, **18**, 1956.
25 A. Bodor, I. Tóth, L. Zékány, I. Bányai, Z. Szabó and G. T. Hefter, Inorganic Reaction Mechanisms Meeting, 97, Debrecen, 1998, Book of Abstracts, p. 23.
26 W. G. Baldwin and D. R. Stranks, *Aust. J. Chem.*, 1968, **21**, 2161.
27 D. Pouli and W. MacF. Smith, *Can. J. Chem.*, 1960, **38**, 567.
28 Z. Szabó, J. Glaser and I. Grenthe, *Inorg. Chem.*, 1996, **35**, 2036.
29 Z. Szabó, W. Aas and I. Grenthe, *Inorg. Chem.*, 1967, **36**, 5369.
30 N. Radic and M. Bralic, *Analyst*, 1990, **115**, 737.
31 B. L. Phillips, W. H. Casey and S. Neugebauer Crawford, *Geochim. Cosmochim. Acta*, 1997, **61**, 3041.
32 T. N. Polynova, N. P. Belskaya, D. Tyurk de Garciya Banus, M. A. Porai-Koshits and L. I. Martinenko, *Z. Struct. Khim.*, 1970, **11**, 164.
33 J. K. Hovey and P. R. Tremaine, *J. Phys. Chem.*, 1985, **89**, 5541.
34 M. Eigen and R. G. Wilkins, *Adv. Chem.*, 1965, **49**, 55.
35 R. M. Fuoss, *J. Am. Chem. Soc.*, 1958, **80**, 5059.
36 D. C. Chandrasekhar and W. L. Jorgensen, *J. Am. Chem. Soc.*, 1984, **106**, 903.
37 D. T. Richens, *The Chemistry of Aqua Ions*, Wiley, Chichester, 1997, p. 143.
38 P.-Å. Bergström, J. Lindgren, M. C. Read and M. Sandström, *J. Phys. Chem.*, 1991, **95**, 7650.
39 W. L. Jorgensen, D. C. Chandrasekhar and J. D. Madura, *J. Chem. Phys.*, 1983, **79**, 926.
40 J. P. Jones and D. W. Margerum, *Inorg. Chem.*, 1969, **8**, 1486.
41 W. DeW. Horrocks, jun., V. K. Arkle, F. J. Liotta and D. R. Sudnick, *J. Am. Chem. Soc.*, 1983, **105**, 3455.
42 J. Blixt, J. Glaser, P. Solymosi and I. Tóth, *Inorg. Chem.*, 1992, **31**, 5288.

Received 6*th April* 1998; *Paper* 8/02603C